Title
Depth Requirements for a Tonne-scale 76Ge Neutrinoless Double-beta Decay Experiment

Authors
Collaboration, The MAJORANA
Aguayo, E
III, FT Avignone
et al.

Publication Date
2011-09-19

Peer reviewed

Depth Requirements for a Tonne-scale ^{76}Ge Neutrinoless Double-beta Decay Experiment

E. Aguayo[o], F.T. Avignone III[q,m], H.O. Back[l,t], A.S. Barabash[c], M. Bergevin[e], F.E. Bertrand[m], M. Boswell[f], V. Brudanin[d], M. Busch[k,t], Y-D. Chan[e], C.D. Christofferson[p], J.I. Collar[i], D.C. Combs[l,t], R.J. Cooper[m], J.A. Detwiler[e], P.J. Doe[h], Yu. Efremenko[s], V. Egorov[d], H. Ejiri[n], S.R. Elliott[f], J. Esterline[k,t], J.E. Fast[o], N. Fields[i], P. Finnerty[j,t], F.M. Fraenkle[j,t], V.M. Gehman[f], G.K. Giovanetti[j,t], M.P. Green[j,t], V.E. Guiseppe[r], K. Gusey[d], A.L. Hallin[a], R. Hazama[n], R. Henning[j,t], A. Hime[f], E.W. Hoppe[o], M. Horton[p], S. Howard[p], M.A. Howe[j,t], R.A. Johnson[h], K.J. Keeter[b], M.E. Keillor[o], C. Keller[r], J.D. Kephart[o], M.F. Kidd[f], A. Knecht[h], O. Kochetov[d], S.I. Konovalov[c], R.T. Kouzes[o], B.D. LaFerriere[o], B.H. LaRoque[f], J. Leon[h], L.E. Leviner[l,t], J.C. Loach[e], S. MacMullin[j,t], M.G. Marino[h], R.D. Martin[e], D.-M. Mei[r], J.H. Merriman[o], M.L. Miller[h], L. Mizouni[q,o], M. Nomachi[n], J.L. Orrell[o], N.R. Overman[o], D.G. Phillips II[j,t], A.W.P. Poon[e], G. Perumpilly[r], G. Prior[e], D.C. Radford[m], K. Rielage[f], R.G.H. Robertson[h], M.C. Ronquest[f], A.G. Schubert[h], T. Shima[n], M. Shirchenko[d], K.J. Snavely[j,t], V. Sobolev[p], D. Steele[f,*], J. Strain[j,t], K. Thomas[r], V. Timkin[d], W. Tornow[k,t], I. Vanyushin[c], R.L. Varner[m], K. Vetter[e,u], K. Vorren[j,t], J.F. Wilkerson[j,t,m], B.A. Wolfe[h], E. Yakushev[d], A.R. Young[l,t], C.-H. Yu[m], V. Yumatov[c], C. Zhang[r]

[a] *Centre for Particle Physics, University of Alberta, Edmonton, AB, Canada*
[b] *Department of Physics, Black Hills State University, Spearfish, SD, USA*
[c] *Institute for Theoretical and Experimental Physics, Moscow, Russia*
[d] *Joint Institute for Nuclear Research, Dubna, Russia*
[e] *Nuclear Science Division, Lawrence Berkeley National Laboratory, Berkeley, CA, USA*
[f] *Los Alamos National Laboratory, Los Alamos, NM, USA*
[g] *Department of Physics, Queen's University, Kingston, ON, Canada*
[h] *Center for Experimental Nuclear Physics and Astrophysics, and Department of Physics, University of Washington, Seattle, WA, USA*
[i] *Department of Physics, University of Chicago, Chicago, IL, USA*
[j] *Department of Physics and Astronomy, University of North Carolina, Chapel Hill, NC, USA*
[k] *Department of Physics, Duke University, Durham, NC, USA*

[*] Corresponding author
Email address: dsteele@lanl.gov (D. Steele)

[l]Department of Physics, North Carolina State University, Raleigh, NC, USA
[m]Oak Ridge National Laboratory, Oak Ridge, TN, USA
[n]Research Center for Nuclear Physics and Department of Physics, Osaka University, Ibaraki, Osaka, Japan
[o]Pacific Northwest National Laboratory, Richland, WA, USA
[p]South Dakota School of Mines and Technology, Rapid City, SD, USA
[q]Department of Physics and Astronomy, University of South Carolina, Columbia, SC, USA
[r]Department of Earth Science and Physics, University of South Dakota, Vermillion, SD, USA
[s]Department of Physics and Astronomy, University of Tennessee, Knoxville, TN, USA
[t]Triangle Universities Nuclear Laboratory, Durham, NC, USA
[u]Alternate address: Department of Nuclear Engineering, University of California, Berkeley, CA, USA

Abstract

Neutrinoless double-beta decay experiments can potentially determine the Majorana or Dirac nature of the neutrino, and aid in understanding the neutrino absolute mass scale and hierarchy. Future ^{76}Ge-based searches target a half-life sensitivity of $>10^{27}$ y to explore the inverted neutrino mass hierarchy. Reaching this sensitivity will require a background rate of <1 count tonne^{-1} y^{-1} in a 4-keV-wide spectral region of interest surrounding the Q value of the decay. We investigate the overburden required to reach this background goal in a tonne-scale experiment with a compact (copper and lead) shield based on Monte Carlo estimates of cosmic-ray background rates. We find that, in light of the presently large uncertainties in these types of calculations, a site with an underground depth $\gtrsim$5200 meters water equivalent is required for a tonne-scale experiment with a compact shield similar to the planned 40-kg Majorana Demonstrator. The required overburden is highly dependent on the chosen shielding configuration and could be relaxed significantly if, for example, a liquid cryogen and water shield, or an active neutron shield were employed. Operation of the Majorana Demonstrator and GERDA detectors will serve to reduce the uncertainties on cosmic-ray background rates and will impact the choice of shielding style and location for a future tonne-scale experiment.

Note added Apr 2013: the peer review process revealed that one of the veto rejection factors (the factor-of-four described on p. 12) needs to be better

established. Our re-evaluation of this parameter to date has not yielded strong support for the value stated in the manuscript, and it will require further study to develop a solid estimate. In the end, these further studies will supersede this aspect of the work described in this manuscript. The new study may or may not lead to the same conclusion regarding the $\gtrsim$5200 meters water equivalent requirement for future tonne-scale ^{76}Ge neutrinoless double beta decay experiments.

Keywords: neutrinoless double-beta decay, Germanium, cosmic rays

1. Introduction

Neutrinoless double-beta ($0\nu\beta\beta$) decay may allow the determination of the Majorana or Dirac nature of the neutrino, and aid in understanding the neutrino absolute mass scale and hierarchy [1, 2, 3, 4, 5, 6]. Guiding principles for extending the Standard Model do not preclude each neutrino mass eigenstate from being identical to its antiparticle, or "Majorana" in nature. The discovery of Majorana neutrinos would have profound theoretical implications for the extension of the Standard Model while yielding insights into the origin of mass and supporting the hypothesis that leptogenesis mechanisms gave rise to the observed baryon asymmetry [7, 8].

Neutrino oscillation experiments [9, 10, 11] indicate that at least one neutrino mass eigenstate has a mass of $\sim$45 meV or more. As a result, in the inverted hierarchy mass spectrum with $m_3 = 0$ meV, the effective Majorana mass of the electron neutrino, $\langle m_{\beta\beta}\rangle$, is between $\sim$15 and $\sim$50 meV depending on the values of the neutrino mixing parameters and Majorana phases. Assuming light Majorana neutrino exchange mediates the decay, the limit on the $0\nu\beta\beta$-decay half-life, $T^{0\nu}_{1/2}$, is related to the limit on the effective neutrino mass as:

$$\frac{1}{T^{0\nu}_{1/2}} = G^{0\nu}|\mathcal{M}^{0\nu}|^2\langle m_{\beta\beta}\rangle^2 \quad (1)$$

where $G^{0\nu}$ is an exactly calculable phase-space factor, and $\mathcal{M}^{0\nu}$ is a nuclear matrix element. The nuclear matrix element is difficult to calculate, and its value is highly model-dependent, but significant progress in reducing the theoretical uncertainty has been made recently [12]. In the case that no signal is observed, the limit that can be placed on $\langle m_{\beta\beta}\rangle$ can be expressed

as:

$$\langle m_{\beta\beta} \rangle = \left[\frac{\text{U.L.}(B)}{ln(2) N_{\text{a}} T \epsilon G^{0\nu} |\mathcal{M}^{0\nu}|^2} \right]^{1/2} \quad (2)$$

where U.L.(B) is the upper limit on the $0\nu\beta\beta$-decay signal given B observed background counts, N_a is the number of $0\nu\beta\beta$-decay candidate atoms, T is the livetime of the experiment, and ϵ is the signal-detection efficiency. As illustrated in Figure 1, exploring the inverted mass hierarchy by searching for $0\nu\beta\beta$ decay in the isotope ^{76}Ge requires a sensitivity of $T^{0\nu}_{1/2} > 10^{27}$ y. This is a challenging goal requiring tonne-years of exposure and a background rate of <1 count tonne^{-1} year^{-1} (ct t^{-1} y^{-1}) in the 4 keV-wide spectral region of interest (ROI) surrounding the $0\nu\beta\beta$-decay Q value ($Q_{\beta\beta}$) of 2039 keV, or a rate more than a factor of 100 lower than was achieved in previous-generation experiments [13, 14].

The MAJORANA [15, 16, 17] and GERDA [18, 19] collaborations are fielding experiments to demonstrate the feasibility of achieving the background rates required for the success of a tonne-scale, ^{76}Ge-based $0\nu\beta\beta$-decay experiment. Lessons learned from both experiments will lead to a single, scalable design utilizing the best aspects of both technologies.

The GERDA collaboration plans to operate (in Phase II of their experiment) a 40-kg array of enriched Ge ($^{\text{enr}}$Ge) crystals immersed inside a cylindrical liquid argon (LAr) cryostat that is 4 m in diameter and ∼5.6 m tall [20]. Surrounding the cryostat is a water tank 10 m in diameter and 8.9 m tall serving as a neutron moderator and gamma-ray shield. The water tank is also a Cherenkov detector equipped with 60 photomultiplier tubes to veto events coincident with through-going muons [21]. The collaboration is also investigating the possibility of instrumenting the LAr volume to serve as an inner active scintillation veto [22]. The background in GERDA is expected to be dominated by cosmogenic and primordial radioisotope impurities in the Ge crystals and small parts near the detectors [23].

The MAJORANA DEMONSTRATOR [15, 16, 17] will be an array of p-type, point-contact (PPC) high-purity Ge diodes [24, 25] housed in two vacuum cryostats built from ultra-pure electroformed Cu (EFCu). Each cryostat will contain 35 diodes, each with mass of about 0.6 kg. Up to 30 kg of the detectors will be built from material enriched to at least 86% ^{76}Ge. A graded, passive shield will be constructed from electroformed and commercial high-purity Cu, high-purity Pb, polyethylene neutron moderator (some of which is borated), and an active plastic scintillator muon veto. The experiment

will be located in a clean room at the 4850-foot level (4300 meters water equivalent, m.w.e.) of the Sanford Underground Laboratory (SUL) at the Homestake mine in Lead, South Dakota. The largest sources of background in the MAJORANA DEMONSTRATOR are expected to be the decay of cosmogenic isotopes in the Ge, primordial isotope decay originating in the detector mounts, cryostat and inner Cu layer of the shield, and inelastic scattering of muon-induced neutrons on the Ge, Cu and Pb.

Both experiments aim to achieve a background rate of 4 ct t^{-1} y^{-1} ROI^{-1} and either confirm a controversial claim of $0\nu\beta\beta$-decay detection in ^{76}Ge [26] or refute the claim and set a limit on the $0\nu\beta\beta$-decay half-life. In particular, the MAJORANA DEMONSTRATOR will set a limit of $T^{0\nu}_{1/2} > 4 \times 10^{25}$ years (90% C.L.) after one year of running. In the case of a tonne-scale experiment based on the MAJORANA DEMONSTRATOR concept, additional reduction in background is achieved via more powerful analysis cuts associated with larger detector arrays, siting the experiment deeper underground, and if necessary, using a thicker layer of EFCu in the shield and fabricating the ^{enr}Ge detectors in an underground laboratory to reduce the amount of cosmogenic activation.

Here we will focus on cosmic-ray backgrounds and discuss the depth requirements for a future tonne-scale experiment. In Sec. 2, we describe the anticipated sources of background and strategies employed for their mitigation. We then quantify the predicted rates of cosmic-ray backgrounds for a tonne-scale experiment in the context of the entire background budget, drawing upon background studies for a generic $0\nu\beta\beta$-decay experiment with a "compact" shield similar to the MAJORANA DEMONSTRATOR, in Sec. 3. In Sec. 4 we derive the depth requirements for a tonne-scale experiment and discuss the interplay between the required depth of the laboratory and the style of shielding.

2. Backgrounds & Mitigation Strategies

Achieving a low background is critical to the search for $0\nu\beta\beta$ decay. In ^{76}Ge, $0\nu\beta\beta$ decay would produce a mono-energetic peak at 2039 keV. With a typical Ge detector resolution of 0.2% FWHM at 2 MeV, less than a fraction of $\sim 2 \times 10^{-15}$ of the continuous two-neutrino double-beta ($2\nu\beta\beta$) decay spectrum contaminates the ROI, making this class of background completely negligible [2]. Any particle with $E > Q_{\beta\beta}$ originating outside of the Ge detector volume depositing a portion of its energy presents a potential background. Even though the excellent inherent energy resolution of Ge detectors

serves to reduce the count rate in the ROI from many sources of background, the detectors themselves and the materials used to fabricate the detector mounts, electronic readout, and shielding must be of extreme radiopurity. The experiment must employ active and passive shielding to reduce external backgrounds originating from natural radioactivity in the cavern walls, and must be sited underground to reduce cosmic-ray backgrounds.

2.1. Depth-dependent backgrounds

Cosmic-ray muons produce electromagnetic (EM) and hadronic particle cascades as they pass through rock, shielding materials, and the Ge diodes. Highly-penetrating neutrons with energies extending up to several GeV can be generated in these cascades. In the MAJORANA DEMONSTRATOR, these neutrons can produce backgrounds via elastic scattering on Ge, Ge(n, n), and inelastic scattering, $(n, n'\gamma)$, on Ge, Pb and Cu. In addition, about a dozen unstable isotopes of Ge, Ga and Zn with half-lives greater than a few seconds and with $Q > Q_{\beta\beta}$ can be produced in the Ge diodes *in situ* by spallation processes. Rarely, muons stop inside the detector and form muonic atoms in which the muon cascades down into the 1S state and either decays via $\mu^- \rightarrow e^- \bar{\nu}_e \nu_\mu$ or is captured by the atomic nucleus via the weak interaction process $\mu^- + p \rightarrow n + \nu_\mu$ [27]. The reaction typically results in nuclear excitations of ∼100 MeV followed by the emission of gamma rays and a number of neutrons with energies typically less than 10 MeV but as high as a few tens of MeV as the daughter nucleus de-excites.

Neutron inelastic scattering interactions producing gamma rays coincident with muon passage through an anti-cosmic veto are relatively easy to eliminate. Of greater concern are un-vetoed neutrons resulting from muon interactions in the walls and other components of the experimental chamber. While the μ-induced neutron flux is typically at least three orders of magnitude lower than the neutron flux from primordial radioactivity at underground depths greater than ∼3000 m.w.e. [28], these neutrons are more penetrating and thus more difficult to shield against. Muon-induced neutron backgrounds can be suppressed by choosing a site deeper underground, or by minimizing the use of high-Z materials in the shield.

As depth increases, the muon energy spectrum becomes harder and the integral flux decreases. As a rule of thumb, the muon flux decreases by about an order of magnitude for every 1500 m.w.e. increase in depth [28]. The integral muon flux at depths greater than ∼1 kilometer water equivalent

(km.w.e.), ϕ_μ, can be parameterized as

$$\phi_\mu(h) = a_0\, e^{-h/0.285} + a_1\, e^{-h/0.698} \tag{3}$$

where h is the flat-overburden-equivalent depth in km.w.e., $a_0 = 68 \times 10^{-6}\,\mathrm{cm}^{-2}\ \mathrm{s}^{-1}$ and $a_1 = 2.1 \times 10^{-6}\,\mathrm{cm}^{-2}\ \mathrm{s}^{-1}$ [28]. Since the muon energy spectrum becomes harder with increasing depth, the μ-induced neutron flux decreases somewhat more slowly with increasing depth and can be parameterized as

$$\phi_n(h) = P_0\left(\frac{P_1}{h}\right)e^{-h/P_1} \tag{4}$$

where $P_0 = (4.0 \pm 1.1) \times 10^{-7}\ \mathrm{cm}^{-2}\ \mathrm{s}^{-1}$ and $P_1 = 0.86 \pm 0.05$ km.w.e. [28]. Furthermore, since the cross section for the *in-situ* production of cosmogenic isotopes increases as a positive power of the muon energy, the rate of cosmogenic isotope production also generally does not decrease as fast as the μ flux with depth. Several studies of μ-induced isotopes in materials ranging from liquid scintillator to Pb have found that the production cross section, σ, goes as

$$\sigma(E_\mu) \propto E_\mu^\alpha \tag{5}$$

where E_μ is the muon energy and α is a constant found to range between 0.50 and 0.93 with a mean value $\langle\alpha\rangle = 0.73 \pm 0.10$ [29]. Using this relation, one can show [28] that the rate of μ-induced cosmogenic isotope production, R_{iso}, scales with depth as

$$\frac{R_{iso}(h=0)}{R_{iso}(h)} = \left(\frac{4\,\mathrm{GeV}}{\langle E_\mu\rangle}\right)^\alpha \frac{\phi_\mu(h=0)}{\phi_\mu(h)} \tag{6}$$

where $\langle E_\mu\rangle$ is the mean muon energy at depth h, which can be written as

$$\langle E_\mu\rangle = \frac{\epsilon_\mu(1 - e^{-bh})}{\gamma_\mu - 2}. \tag{7}$$

The parameters ϵ_μ, b and γ_μ depend on the muon energy spectrum in the atmosphere, muon energy loss processes in rock, and local rock density and composition. Values provided by Lipari & Stanev [30] ($b = 0.383$ / km.w.e., $\gamma_\mu = 3.7$ and $\epsilon_\mu = 618$ GeV) and Battistoni et al. [31] ($b = 0.4$ / km.w.e., $\gamma_\mu = 3.77$ and $\epsilon_\mu = 693$ GeV) both agree with the measured value of the mean muon energy at the Gran Sasso National Laboratory (LNGS) [32].

2.2. External & intrinsic backgrounds

Significant backgrounds arise from naturally-occurring primordial radioactivity present in materials, including in the walls of the underground cavern. One of the isotopes in the ^{232}Th decay chain, ^{208}Tl, is of particular concern, since it decays with the emission of a 2615-keV gamma ray, well above $Q_{\beta\beta}$ for ^{76}Ge. An isotope in the ^{238}U decay chain, ^{214}Bi, also decays with the emission of gamma rays with energies above $Q_{\beta\beta}$. Radon and the plate-out of its daughters inside the shield and cryostat present a variety of potential α, β and γ backgrounds. A massive bulk shield composed of radiologically clean material and a Rn exclusion box surrounding the detector systems has been repeatedly demonstrated to greatly reduce primordial gamma-ray backgrounds originating externally to the shield.

Neutrons resulting from the decay of primordial isotopes in the cavern walls, such as from the spontaneous fission of ^{238}U or from natural alpha emitters via (α, n) reactions, are also of concern. These neutrons can produce gamma rays with energies above $Q_{\beta\beta}$ through inelastic scattering and capture processes in the shielding materials or in the detectors themselves. With a maximum energy of $\sim$10 MeV, these neutrons can be substantially suppressed by incorporating a hydrogenous neutron absorber into the bulk shield.

Great care must also be taken to minimize the radioactive contaminants present in the components used inside the shield. Copper has become a material of choice for the construction of ultra-low-background detectors because of its lack of naturally-occurring radioisotopes, its excellent physical properties, and the ability to purify it to a high degree via electrodeposition [33, 34, 35]. One must ensure that it does not have significant quantities of cosmogenic radioisotopes, the most troublesome of which is ^{60}Co, generated by (n, α) reactions on ^{63}Cu. The strategy employed by MAJORANA to mitigate this background is to electroform Cu parts underground.

Germanium detectors have the advantage that problematic radioisotopes are effectively removed during the detector production process. The cosmogenic isotope ^{68}Ge is removed during the enrichment of the Ge material. Impurities of U and Th, as well as cosmogenic ^{60}Co, are effectively removed during the zone refinement and crystal pulling stages. The relatively long-lived cosmogenic isotopes ^{60}Co ($T_{1/2} = 5.3$ y) and ^{68}Ge ($T_{1/2} = 271$ d) are produced via cosmic-ray spallation in Ge. With a Q value of 2.8 MeV, ^{60}Co β decay contributes to the background continuum. Although ^{68}Ge decays by electron capture with $Q < Q_{\beta\beta}$, its daughter isotope, ^{68}Ga, has a half-life

of 68 minutes and decays predominantly by β^+ emission with a Q value of 2.9 MeV. The K- and L-shell X rays from the ^{68}Ge decay can potentially be used to tag the subsequent ^{68}Ga decay and veto any events occurring within the time span of a few ^{68}Ga half-lives. In addition, ^{68}Ge has a half-life much shorter than the expected ∼10-year time scale of a tonne-scale experiment. More direct mitigation of cosmogenic backgrounds must be achieved by carefully limiting the aboveground exposure of the enriched material and completed detectors to cosmic rays, or (more ideally) by conducting as much of the detector fabrication process as practicable in an underground laboratory [36].

3. Simulations & Background Studies

In this section we synthesize the results from a number of simulations and background studies to estimate the total background for a tonne-scale $0\nu\beta\beta$-decay experiment with a compact shield. The rate of cosmic-ray backgrounds as a function of depth for ^{76}Ge-based $0\nu\beta\beta$-decay experiments was studied by Mei & Hime [28] with an extensive FLUKA- and GEANT3-based custom Monte Carlo (MC) calculation. In Sec. 3.1 we summarize the salient results and use the scaling relations in Sec. 2.1 to derive cosmic-ray background rates for an experiment situated at the 4850-foot level of SUL. Additional results attained using the same framework but performed after the publication of Mei & Hime [28] are used to describe how modifications in the thickness of neutron shielding and muon veto efficiency change the results. In Sec. 3.2 we describe our simulations of a 60-kg detector module with a compact shield similar to the MAJORANA DEMONSTRATOR conducted within the MaGe [37] simulation framework. Based on the simulation, we use a parametric model to link material radiopurity goals for various shield and detector components to background counts in $0\nu\beta\beta$-decay ROI, taking into account analysis cut efficiencies, to demonstrate that a rate of ∼1 ct t^{-1} y^{-1} ROI^{-1} can be achieved in a tonne-scale experiment.

3.1. Cosmic-ray muon-induced backgrounds

Simulated cosmic-ray background rates, including direct contributions from untagged muons, muon capture, untagged μ-induced fast neutron elastic and inelastic scattering, and cosmogenic radioactive isotope production *in situ*, have been reported by Mei & Hime [28]. Their work employed FLUKA to simulate the interactions of cosmic ray muons in the rock surrounding the

experimental apparatus. The muon energies and angular distributions were sampled from empirical parameterizations. The generated spallation neutrons were propagated to the cavern walls, at which point they were booked in histograms to be used in event generators for a GEANT3-based simulation of the detector response, using Hauser-Feshback theory to calculate neutron inelastic scattering cross sections. The simulated experimental set-up included a 60-kg array of enriched Ge crystals inside a compact shield with a 10-cm-thick inner Cu layer followed by 40 cm of Pb, 10 cm of polyethylene, and an outer active muon veto with 90% efficiency. To enable an easy comparison to other experiments, the simulated set-up was situated at the depth of LNGS (3100 m.w.e., flat-overburden-equivalent). Mei & Hime [28] found that the dominant μ-induced contribution to the background is from fast neutron elastic and inelastic scattering on Ge. The background rates of the simulated processes are summarized in Table 1.

Before discussing how the results scale with changes in the shield configuration, it is necessary at the outset to mention that MC estimates of μ-induced background rates at great depths underground are fraught with significant uncertainty. An uncertainty of 10-15% on the muon flux at depth is attributed to the uncertainties in our knowledge of primary muon flux and energy spectrum in the atmosphere [28, 38]. Uncertainty in the effective depth of the underground laboratory results in 30% uncertainty in the muon flux normalization for the case of the 4850-foot level of SUL (4300 $\pm$ 200 m.w.e. [28]). Kudryavtsev et al. [38] compared differences in muon propagation for two different types of rock composition ("standard rock" and Modane rock) and found a 15% change in the muon flux normalization at a depth of 5000 m.w.e., but no significant change in the mean muon energy. Adding these uncertainties in quadrature results in a 37% uncertainty on the muon flux normalization at 4300 m.w.e. depth.

Uncertainties on the μ-induced neutron fluxes are larger. The μ-induced neutron yield in materials with $Z < 40$ disagrees by 40% between GEANT4 and FLUKA and by a factor of 2 for high-Z materials such as Pb [39]. While neutron yields in FLUKA are higher than in GEANT4, comparison to experimental data indicates that both codes under predict neutron yields in light materials, and probably do so for Pb as well [39]. We therefore include a factor-of-two uncertainty on the μ-induced neutron yield when calculating our background rates. Uncertainties due to neutron tracking in the Monte Carlo are typically taken to be $\sim$20% based on the level of agreement between different codes [40]. Mei & Hime [28] note that neutron backscattering off of

the walls of the experimental cavern can result in a factor of 2 to 3 change in the neutron flux incident on the shielding depending on the exact dimensions of the cavern and shield. Mei & Hime [28] included the effects of neutron backscattering in their simulations for a cavern with dimensions of 30 $\times$ 6.5 $\times$ 4.5 m^3. We take the uncertainty on the neutron flux due to the effect of backscattering to be 150%, and note that for a larger cavern, the contribution of backscattering to the total muon-induced background is expected to be smaller. Adding the logarithms of the uncertainties in quadrature, we find a total uncertainty on the muon-induced neutron flux of a factor of 3.2.

With these limitations in mind, we scale the Mei & Hime [28] results to reflect the μ-induced background rates in a more realistic representation of the planned MAJORANA DEMONSTRATOR shield configuration. The major differences are: a thicker (30-cm) layer of polyethylene neutron moderator, a 99%-efficient muon veto, and an overburden corresponding to the depth of the 4850-foot level at SUL (4300 $\pm$ 200 m.w.e.). The fraction of unvetoed direct muon hits is decreased by a factor of 10 on account of the more efficient anti-cosmic veto. According to Eqs. 3 and 4 we also gain reduction factors of 5.9 and 5.6 for the direct muon flux and μ-induced neutron flux, respectively, on account of the greater depth. Since the "Others" category in Table 1 includes *in-situ* production of cosmogenic isotopes in addition to some processes whose rates decrease more quickly with depth, we conservatively use Eq. 6 to quantify the depth dependence of backgrounds in that category, resulting in a reduction factor of 5.3. We have assumed that the effects of changes in the energy spectrum of neutrons penetrating through the thicker layer of polyethylene can be neglected in comparison to the large uncertainties on the overall μ-induced neutron flux. Simulations performed after the publication of Mei & Hime [28] using the same framework showed that increasing the thickness of the polyethylene from 10 cm to 30 cm reduces the μ-induced fast neutron flux penetrating the shield by a factor of two, and that the more efficient anti-cosmic shield decreases the number of untagged neutrons from muons that do not cross the detector by a factor of 1.8. Even though most μ-induced neutrons are accompanied by the muon itself, the detection efficiency is much lower for those that are not, and so we also conservatively use this factor to describe the improvement in veto efficiency for all μ-induced neutrons.

Muon-induced neutrons emerging from the cavern wall are typically accompanied by electromagnetic (EM) cascades. The Mei & Hime [28] simulation treated the generation of μ-induced neutrons in the rock separately from

their propagation into and through the detector shielding. Simulations of the EDELWEISS experiment, a Ge-based dark matter experiment with a compact shield design similar to that envisioned here, indicate that including EM cascades improves the veto efficiency by almost an order of magnitude [41]. Given the differences in the backgrounds relevant for dark matter searches and $0\nu\beta\beta$ decay, we use this value as an upper limit and conservatively choose a factor of four background reduction, with a factor-of-two uncertainty, to correct for the missing EM cascades in the Mei & Hime [28] simulations. The corresponding uncertainty introduced on the background rates is 60%, much smaller than the uncertainty due to neutron yield and tracking. By including this factor, any depth-dependent change in neutron veto efficiency due to the μ-induced neutron energy spectrum becoming harder with increasing depth does not significantly change the results. The scaling factors used to modify the Mei & Hime [28] results as discussed above are summarized in Table 2.

Mei & Hime [28] state that the application of analysis cuts can potentially reduce the total μ-induced neutron background rates by a factor of $\sim$7.4. However, this factor should decrease as the anti-cosmic veto efficiency increases from 90%, as assumed in Mei & Hime [28], to 99% as assumed in this work. The granularity and pulse-shape-analysis (PSA) cuts (see Sec. 3.2) are most effective for rejecting high-multiplicity events, but as the veto efficiency increases, the average multiplicity of events that do not trigger the veto decreases. Based on our experience simulating other backgrounds, we expect analysis cuts to contribute at least a factor 2.5 reduction (cut efficiency of 40%) in the rate of μ-induced neutron backgrounds. Assuming this corresponds to an upper limit on the cut efficiency, and assuming the factor of 7.4 from Mei & Hime [28] corresponds to a lower limit (14% cut efficiency), we will assume an analysis cut efficiency of 25%, with an uncertainty of 60%.

Including the effects of analysis cuts and logarithmically adding in quadrature the uncertainties on the cut efficiencies (60%), muon flux normalization (37%), neutron yield and tracking (a factor of 3.2), and the scaling factors introduced to adjust the Mei & Hime [28] results (60%), the total μ-induced background rate for an experiment with a compact shield configuration situated at 4300 m.w.e. is 0.33 ct t^{-1} y^{-1} ROI^{-1} with an uncertainty of a factor of $\sim$4.

3.2. MaGe simulations

MaGe is an object-oriented simulation package based on ROOT [42] and the GEANT4 toolkit [43, 44] optimized for simulations of low-background

Ge detector arrays [37]. MaGe is developed and maintained jointly by the MAJORANA and GERDA collaborations. Simulations performed to reproduce experimental data taken with a number of different detectors and radioactive sources generally reproduce spectral features – such as relative peak heights, peak to Compton ratios, and Compton scattering multiplicity – to within 5-10% [37]. In cases where GEANT4 has been shown to perform inadequately when compared to data, such as in neutron production from cosmic-ray muons and neutron inelastic scattering [45], efforts are underway within the MAJORANA, GERDA, and GEANT collaborations to correct or compensate for the inadequacies.

Neutrinoless double-beta decay results in the emission of two electrons, and because these electrons travel very short distances ($\sim$1 mm) in Ge, their energy depositions are effectively *single-site* events. In contrast, most backgrounds arise from the interaction of gamma rays in the detector. Gamma rays with energies at or above $Q_{\beta\beta}$, with a mean distance of centimeters between Compton scatters in Ge, are likely to deposit only a portion of their energy. If the energy deposited is within a few keV of $Q_{\beta\beta}$, the interaction represents a background to the $0\nu\beta\beta$-decay signal. Such interactions are typically *multi-site* energy depositions. Multi-site events can be identified and rejected if the multiple scatters occur in more than one crystal in a tightly-packed array. This *granularity* technique is estimated to contribute a factor 2 to 5 suppression of multi-site events, depending on the origin of the background. Modern signal digitization techniques also allow for the discrimination between single-site and multi-site event topologies in a single crystal. P-type, point-contact detectors are particularly suitable for the application of these techniques. Measurements indicate that PSA techniques applied to data from PPC detectors can reject >90% of multi-site background events while retaining >90% of single-site events [46, 47].

We have employed the MaGe simulation package to determine the background rates from each major background source discussed in Sec. 2 for generic ^{76}Ge-based $0\nu\beta\beta$-decay experiments. The simulated geometries included 3-, 9-, 21- and 57-detector arrays of 1.05-kg, semi-coaxial Ge crystals, and a 35-crystal array of 560-g PPC detectors. For each geometry, the Cu mounts, front-end read-out electronics near the detectors, and cables were simulated inside a Cu cryostat. The detector module was enclosed inside a compact shield of Cu and Pb corresponding to the baseline thicknesses for the MAJORANA DEMONSTRATOR described above. Using MC calculations of the detector response, measured or targeted levels of impurities can be

linked to background rates in the 4-keV-wide ROI. For example, in the ^{232}Th and ^{238}U decay chains, we focus on the two radionuclides that have gamma-ray lines above $Q_{\beta\beta}$: ^{208}Tl and ^{214}Bi. The estimates include component- and background-specific suppression factors, including those from the granularity and PSA cuts, and for ^{68}Ga decays, a time-correlation cut corresponding to five ^{68}Ge half lives. The granularity cut is applied to any event in which more than one detector is triggered and records >5 keV of energy deposited. Since our PSA software was not fully implemented at the time when the simulations were run, the PSA background suppression capabilities were estimated by applying a heuristic based on the charge-drift properties and signal characteristics of PPC detectors, including the impact of noise and readout bandwidth. PSA simulations were subsequently performed and the results were found to be consistent with the heuristic-based analysis. The results for the 57-crystal array (the size envisioned for a tonne-scale experiment) are summarized in Table 3.

Based on the absence of clear α peaks in the Heidelberg-Moscow data [13], we place upper limits on the ^{238}U and ^{232}Th contamination in the Ge crystals of $<1\times10^{-15}$ g/g and $<4\times10^{-15}$ g/g, respectively, corresponding to a background rate of <0.30 ct t^{-1} y^{-1} ROI^{-1} from all decay processes in the two decay chains, assuming secular equilibrium. We estimate a background rate of <0.04 ct t^{-1} y^{-1} ROI^{-1} from the decay of cosmogenic ^{68}Ge and ^{60}Co in the Ge crystals assuming the $^{\rm enr}$Ge material is limited to a maximum of 100 d of sea-level-equivalent cosmic-ray exposure. Our estimate includes the effects of PSA and granularity cuts, and the veto of any events occuring within five ^{68}Ga half-lives after the observation of a K-shell X ray from the decay of ^{68}Ge. The largest contribution to the total background (0.46 ct t^{-1} y^{-1} ROI^{-1}) is expected to originate from the EFCu portion of the shield and the cryostats. Additional sources of background present inside the shield include the detector mounts, front-end electronics, cables, and other small parts, contributing <0.14 ct t^{-1} y^{-1} ROI^{-1}.

By simulating different background sources under a variety of detector shielding configurations, we were able to parametrically extrapolate background estimates for different shielding designs. By doubling the thickness of EFCu shielding relative to that proposed for the Majorana Demonstrator, we estimate that backgrounds in a tonne-scale experiment from an outer, commercial Cu shielding layer would be ∼0.02 ct t^{-1} y^{-1} ROI^{-1}. In this configuration, backgrounds from natural radioactivity in the Pb would be negligible (<0.02 ct t^{-1} y^{-1} ROI^{-1}). The effectiveness of the shield and

neutron moderator limits the background from external gamma rays and neutrons from the cavern walls to $\sim$0.05 ct t^{-1} y^{-1} ROI^{-1}.

The total depth-independent background rate of $\lesssim$1.1 ct t^{-1} y^{-1} ROI^{-1} carries an uncertainty of 30%. We note that the sum of depth-independent backgrounds leaves no room for depth-dependent backgrounds if the background goal of <1 ct t^{-1} y^{-1} ROI^{-1} is to be achieved.

4. Depth Requirements

A tonne-scale, ^{76}Ge-based $0\nu\beta\beta$-decay experiment must strive to make μ-induced backgrounds negligible compared to the $\sim$1 ct t^{-1} y^{-1} ROI^{-1} expected from depth-independent backgrounds. At a depth of 4300 m.w.e., the rate of μ-induced neutron backgrounds for a compact shield configuration similar to the MAJORANA DEMONSTRATOR is expected to be $\sim$0.3 ct t^{-1} y^{-1} ROI^{-1} after analysis cuts, but with an uncertainty of a factor of 4, dominated by uncertainties associated with the μ-induced neutron yield in high-Z materials and the effects of neutron backscattering. A target μ-induced background rate of 0.1 ct t^{-1} y^{-1} ROI^{-1} implies a depth requirement of $\gtrsim$5200 m.w.e. assuming the expectation value of the estimated background rate. However, given the large uncertainty, an even deeper location would be preferred to mitigate the associated risk. Figure 2 illustrates this requirement in the context of several existing and possible future underground laboratories.

Table 1 indicates that the depth-dependent background for an experiment with a compact, high-Z shield configuration is dominated by μ-induced neutron inelastic scattering on Cu and Pb components of the shield. Eliminating high-Z materials close to the Ge detectors reduces this background contribution and can significantly relax the depth requirement. This is the approach taken by GERDA. The rates of μ-induced backgrounds in GERDA at the depth of LNGS (3100 m.w.e.) have been calculated using a MC simulation by Pandola et al. [40]. The production and subsequent decay of cosmogenic isotopes in the Ge crystals and the LAr volume was found to be the limiting depth-dependent background with a rate of $\sim$0.8 ct t^{-1} y^{-1} ROI^{-1}, including a conservative accounting for the effects of analysis cuts. The decay of ^{77}Ge and ^{77m}Ge produced by neutron capture of thermalized μ-induced neutrons produced in the shield volume was found to be the dominant contribution. The authors assign statistical and systematic uncertainties of $\sim$20% and 45%, respectively, to the estimated rate. The lower systematic error compared to our estimate for a compact shield is possible because for materials

with $Z < 40$, the predicted neutron yields are in closer agreement between different MC codes than those for Pb, and backscattering neutrons in the cavern are not expected to contribute significantly to the background. Pandola et al. [40] also found that the μ-induced background rates are an order of magnitude smaller in the case that liquid nitrogen is used in the shield in place of LAr [40] because the μ-induced particle showers do not develop to the same extent as in LAr.

The μ-induced background rate in GERDA would be reduced by a factor $\sim$5 to $\sim$0.15 ct t^{-1} y^{-1} ROI^{-1} at the depth of SUL according to Eq. 6. When comparing this rate to our estimate of 0.33 ct t^{-1} y^{-1} ROI^{-1} for a compact shield, we must keep in mind that the uncertainty is significantly smaller, and that the estimated rate for GERDA is an upper limit since the assumed analysis cut efficiency for the ^{77}Ge background is probably conservative [40].

The depth requirement for an experiment with a compact shield configuration is driven in large part by the present uncertainty associated with MC predictions of neutron yields in high-Z materials. The depth requirement can be relaxed significantly for a low-Z shield configuration since the associated μ-induced background rates for low-Z configurations are lower and have smaller uncertainties. In particular, for a GERDA-style experiment using LN_2 for shielding, μ-induced backgrounds would be negligible at the depth of the SUL 4850-foot level. It should be noted, however, that such a shield configuration would be more technically complex, would require much more space, and could present significant oxygen deficiency and other safety hazards.

5. Conclusions

The Majorana and GERDA collaborations are developing experiments based on different shielding techniques to demonstrate that a tonne-scale, ^{76}Ge-based $0\nu\beta\beta$-decay experiment can achieve the extremely low background rates necessary to accomplish the science goals. Achieving the desired scientific impact depends crucially upon reducing the background rate to $\lesssim$1 ct t^{-1} y^{-1} ROI^{-1}. Even with the utmost attention to cleanliness and the radiopurity of construction materials, a tonne-scale experiment will likely have to contend with a background rate of $\sim$1 ct t^{-1} y^{-1} ROI^{-1} from impurities in the detectors, their mounts and cables, and the shield. Therefore, a tonne-scale experiment should strive to make negligible all μ-induced backgrounds.

The planned depth of 4300 m.w.e. for the MAJORANA DEMONSTRATOR is ideal in that μ-induced backgrounds are expected to be measureable but not dominant, thus enabling a proper assessment of backgrounds from various different sources. We have shown that μ-induced backgrounds are expected to be of significant concern for a tonne-scale experiment with a shield similar to that of the MAJORANA DEMONSTRATOR if it were operated at the same depth.

A tonne-scale $0\nu\beta\beta$-decay experiment with a compact shield will likely need to be located at a depth of $\gtrsim$5200 m.w.e. Based on our current knowledge, an even deeper location is preferred to mitigate the risks arising from large uncertainties in the estimated μ-induced background rates stemming in large part from poor knowledge of μ-induced neutron yields in high-Z materials. We note that the largest single uncertainty in the background rate corresponds to neutron backscattering whose effects are highly dependent on the cavern and experimental geometry. For a cavern larger than that simulated in Mei & Hime [28], this uncertainty should contribute to a downward change in the estimated muon-induced background rate. The depth requirement could also be significantly relaxed if a low-Z shielding configuration or an active neutron veto system were employed.

The eventual choice of the location for a tonne-scale experiment will involve a careful analysis of the backgrounds achieved in the MAJORANA DEMONSTRATOR and GERDA together with an evaluation of the complex interplays between the cosmic-ray shielding afforded by depth, technical feasibility, and background suppression capability of alternative shield designs.

Acknowledgments

We acknowledge support from the Office of Nuclear Physics in the DOE Office of Science under grant numbers DE-AC02-05CH11231, DE-FG02-97ER41041, DE-FG02-97ER41033, DE-FG02-97ER4104, DE-FG02-97ER41042, DE-SCOO05054, DE-FG02-10ER41715, and DE-FG02-97ER41020. We acknowledge support from the Particle and Nuclear Astrophysics Program of the National Science Foundation through grant numbers PHY-0919270, PHY-1003940, 0855314, and 1003399. We gratefully acknowledge support from the Russian Federal Agency for Atomic Energy. We gratefully acknowledge the support of the U.S. Department of Energy through the LANL/LDRD Program. N. Fields is supported by the DOE/NNSA SSGF program.

References

[1] J. Schechter, J. W. F. Valle, Neutrinoless double-beta decay in SU(2) x U(1) theories, Phys. Rev. D 25 (1982) 2951.

[2] S. R. Elliott, P. Vogel, Double beta decay, Ann. Rev. Nucl. Part. Sci. 52 (2002) 115–151.

[3] A. S. Barabash, Double-beta-decay experiments: Present status and prospects for the future, Phys. Atom. Nucl. 67 (2004) 438–452.

[4] H. Ejiri, Double beta decays and neutrino masses, J. Phys. Soc. Jpn. 74 (2005) 2101–2127.

[5] F. T. Avignone, G. S. King, Y. G. Zdesenko, Next generation double-beta decay experiments: Metrics for their evaluation, New J. Phys. 7 (2005) 6.

[6] F. T. Avignone, III, S. R. Elliott, J. Engel, Double beta decay, majorana neutrinos, and neutrino mass, Rev. Mod. Phys. 80 (2008) 481–516.

[7] M. Fukugita, T. Yanagida, Barygenesis without grand unification, Phys. Lett. B 174 (1986) 45–47.

[8] S. R. Elliott, J. Engel, Double beta decay, J. Phys. G30 (2004) R183.

[9] Y. Ashie et al., Measurement of atmospheric neutrino oscillation parameters by Super-Kamiokande I, Phys. Rev. D 71 (2005) 112005.

[10] M. H. Ahn et al., Measurement of neutrino oscillation by the K2K experiment, Phys. Rev. D 74 (2006) 072003.

[11] P. Adamson et al., Measurement of neutrino oscillations with the MINOS detectors in the NuMI beam, Phys. Rev. Lett. 101 (2008) 131802.

[12] V. A. Rodin et al., Assessment of uncertainties in QRPA $0\nu\beta\beta$-decay decay, Nucl. Phys. A766 (2006) 107–131, errata in Nucl. Phys. A793 (2007) 213-215.

[13] L. Baudis et al., New limits on dark-matter weakly interacting particles from the Heidelberg-Moscow experiment, Phys. Rev. D 59 (1998) 022001.

[14] C. E. Aalseth et al., IGEX ^{76}Ge neutrinoless double-beta decay experiment: Prospects for next generation experiments, Phys. Rev. D 65 (2002) 092007.

[15] S. R. Elliott et al., The MAJORANA project, J. Phys. Conf. Ser. 173 (2009) 012007.

[16] R. Henning et al., The MAJORANA DEMONSTRATOR: An R&D project towards a tonne-scale germanium neutrinoless double-beta decay search, AIP Conf. Proc. 1182 (2009) 88–91, paper submitted to the 10th Conference on the Intersections of Particle and Nuclear Physics (CIPANP 2009).

[17] C. E. Aalseth et al., The MAJORANA experiment, Nucl. Phys. B 217 (2011) 44, presentation at the NOW 2010 meeting.

[18] I. Abt et al., A new Ge-76 double beta decay experiment at LNGS, arXiv:hep-ex/0404039v1.

[19] S. Schönert et al., The GERmanium Detector Array (GERDA) for the search of neutrinoless $\beta\beta$ decays of ^{76}Ge at LNGS, Nuc. Phys. B - Proc. Sup. 145 (2005) 242–245.

[20] I. Barabanov et al., Shielding of the GERDA experiment against external gamma background, Nucl. Instrum. Meth. A 606 (2009) 790–794.

[21] M. Knapp et al., The GERDA muon veto Cherenkov detector, Nucl. Instrum. Meth. A 610 (2009) 280 – 282.

[22] P. Peiffer et al., Pulse shape analysis of scintillation signals from pure and xenon-doped liquid argon for radioactive background identification, Journal of Instrumentation 3 (2008) 8007.

[23] D. Budjás et al., Gamma-ray spectrometry of ultra low levels of radioactivity within the material screening program for the GERDA experiment, Appl. Radiat. Isot. 67 (2009) 755–758.

[24] P. Luke et al., Low capacitance large volume shaped-field germanium detector, IEEE Trans. Nucl. Sci. 36 (1989) 926 –930.

[25] P. S. Barbeau, J. I. Collar, O. Tench, Large-Mass Ultra-Low Noise Germanium Detectors: Performance and Applications in Neutrino and Astroparticle Physics, JCAP 0709 (2007) 009.

[26] H. V. Klapdor-Kleingrothaus, I. V. Krivosheina, The evidence for the observation of $0\nu\beta\beta$ decay: The identification of $0\nu\beta\beta$ events from the full spectra, Mod. Phys. Lett. A21 (2006) 1547–1566.

[27] D. F. Measday, The nuclear physics of muon capture, Phys. Rep. 354 (2001) 243–409.

[28] D.-M. Mei, A. Hime, Muon-induced background study for underground laboratories, Phys. Rev. D 73 (2006) 053004.

[29] T. Hagner et al., Muon-induced production of radioactive isotopes in scintillation detectors, Astropart. Phys. 14 (2000) 33–47.

[30] P. Lipari, T. Stanev, Propagation of multi-TeV muons, Phys. Rev. D 44 (1991) 3543–3554.

[31] G. Battistoni et al., Study of photonuclear interaction of muons in rock with the MACRO experiment, arXiv:hep-ex/9809006v1.

[32] M. Ambrosio et al., Measurement of the residual energy of muons in the Gran Sasso underground laboratories, Astropart. Phys. 19 (2003) 313–328.

[33] R. Brodzinski et al., Low-background germanium spectrometry the bottom line three years later, J. Radioanal. Nucl. Chem. 193 (1995) 61–70.

[34] E. Hoppe et al., Cleaning and passivation of copper surfaces to remove surface radioactivity and prevent oxide formation, Nucl. Instrum. Meth. A 579 (2007) 486.

[35] E. Hoppe et al., Use of electrodeposition for sample preparation and rejection rate prediction for assay of electroformed ultra high purity copper for ^{232}Th and ^{238}U prior to inductively coupled plasma mass spectrometry (ICP/MS), J. Radioanal. Nucl. Chem. 277 (2008) 103–110.

[36] D.-M. Mei et al., Underground high-purity germanium crystal growth for DUSEL experiment, J. Cryst. Growth, submitted (2011).

[37] M. Boswell et al., MaGe - a Geant4-based Monte Carlo application framework for low-background germanium experiments, IEEE Trans. Nucl. Sci. 58 (2011) 1212.

[38] V. A. Kudryavtsev, N. J. C. Spooner, J. E. McMillan, Simulations of muon-induced neutron flux at large depths underground, Nucl. Instrum. Meth. A 505 (2003) 688–698.

[39] H. M. Araújo et al., Muon-induced neutron production and detection with GEANT4 and FLUKA, Nucl. Instrum. Meth. A 545 (2005) 398–411.

[40] L. Pandola et al., Monte Carlo evaluation of the muon-induced background in the GERDA double beta decay experiment, Nucl. Instrum. Meth. A 570 (2007) 149–158.

[41] M. Horn, Simulations of the muon-induced neutron background of the EDELWEISS-II experiment for Dark Matter search, Ph.D. thesis, Universität Karlsruhe (2007).

[42] R. Brun, F. Rademakers, ROOT: An object oriented data analysis framework, Nucl. Instrum. Meth. A 389 (1997) 81–86.

[43] S. Agostinelli et al., GEANT4: A simulation toolkit, Nucl. Instrum. Meth. A 506 (2003) 250–303.

[44] J. Allison et al., GEANT4 developments and applications, IEEE Trans. Nucl. Sci. 53 (2006) 270–278.

[45] M. Marino et al., Validation of spallation neutron production and propagation within GEANT4, Nucl. Instrum. Meth. A 582 (2007) 611–620.

[46] R. J. Cooper et al., A Pulse Shape Analysis technique for the MAJORANA experiment, Nucl. Instrum. Meth. A 629 (2011) 303–310.

[47] R. González de Orduña et al., Pulse shape analysis to reduce the background of BEGe detectors, J. Radioanal. Nucl. Chem. 286 (2010) 477–482.

[48] J. Suhonen, O. Civitarese, Weak-interaction and nuclear-structure aspects of nuclear double beta decay, Physics Reports 300 (1998) 123 – 214.

[49] F. Šimkovic et al., $0\nu\beta\beta$-decay nuclear matrix elements with self-consistent short-range correlations, Phys. Rev. C 79 (2009) 055501.

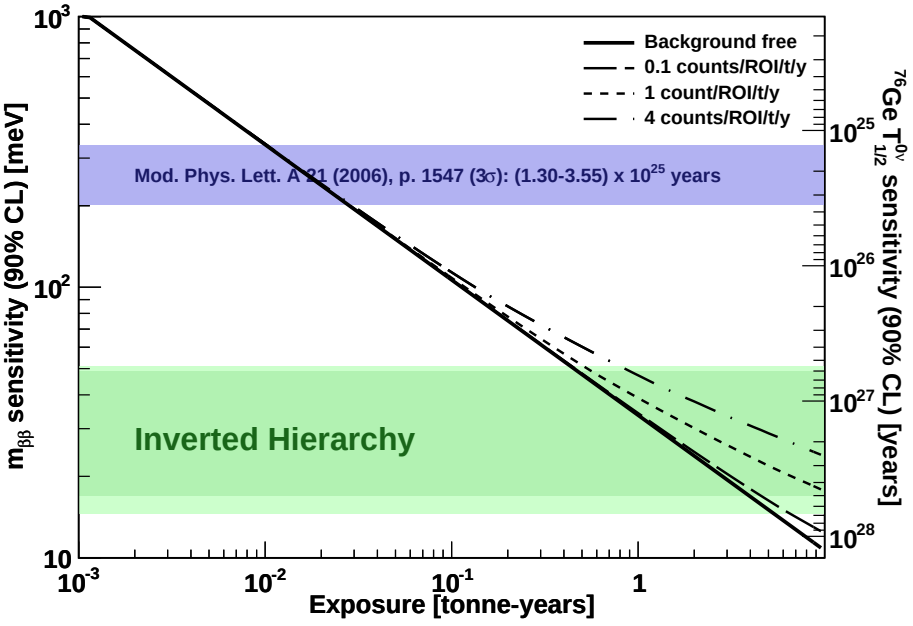

Figure 1: The sensitivity of a search for $0\nu\beta\beta$ decay using 86%-enriched ^{76}Ge as a function of background rate and exposure calculated according to equations 1 and 2. We take the signal detection efficiency, ϵ, to be 68% to account for the effects of analysis cuts. The exposure is defined to as the product of the active mass of the detectors and the live time of the experiment. The phase space factor $G^{0\nu}$ is taken from Ref. [48] and the conversion from half-life to $\langle m_{\beta\beta}\rangle$ is performed using a QRPA-calculated nuclear matrix element [49]. The dark-green band indicates the range of $\langle m_{\beta\beta}\rangle$ in the inverted mass hierarchy for the full range of CP-violating phases, while the light-green bands take into account uncertainties in the measured neutrino oscillation parameters. The half-life corresponding to the recent claim of $0\nu\beta\beta$-decay detection [26] is shown in blue.

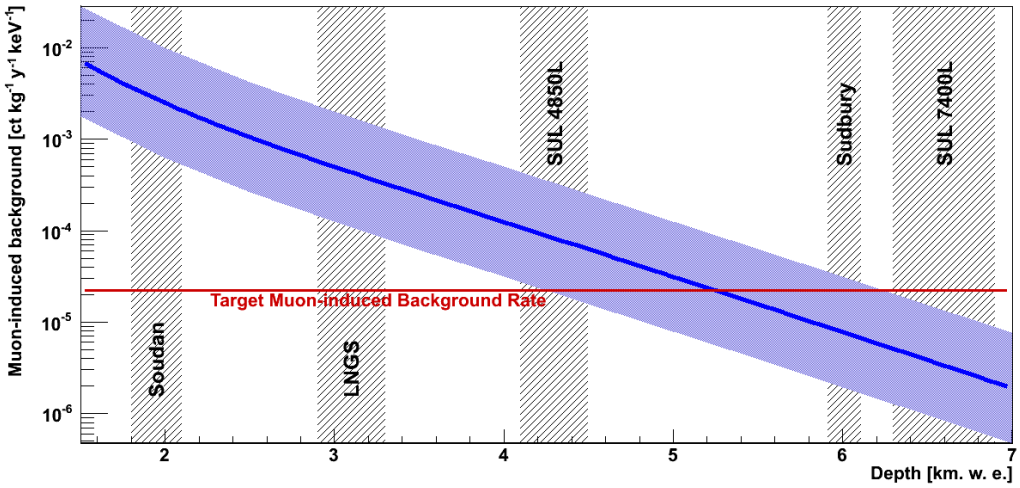

Figure 2: The μ-induced background rate for a tonne-scale $0\nu\beta\beta$-decay experiment with a compact shield is plotted according to Eq. 3, normalized to a rate of 0.33 ct t^{-1} y^{-1} ROI^{-1} at 4300 m.w.e. (see Table 1 and Sec. 3.1). The blue band represents a factor of 4 uncertainty in the background rate. The diagonally-shaded bands show the effective depths (and associated uncertainties according to Ref. [28]) for several underground laboratories. The target μ-induced background rate corresponds to 0.1 ct t^{-1} y^{-1} ROI^{-1}.

Reaction	BG in Ref. [28]	Scaled BG
$^{76}\mathrm{Ge}(n, n'\gamma)$	40	0.49
$^{74}\mathrm{Ge}(n, n'\gamma)$	8.0	0.10
$\mathrm{Cu}(n, n'\gamma)$	7.6	0.094
$^{208}\mathrm{Pb}(n, n'\gamma)$	14	0.17
$\mathrm{Ge}(n, n)$	14	0.17
μ hits	10	0.17
Others	9.6	0.13
Total	**100**	**1.3**

Table 1: Muon-induced background rates for a generic $0\nu\beta\beta$-decay experiment with a compact shield similar to the planned MAJORANA DEMONSTRATOR operating at Gran Sasso (3100 m.w.e.) reported in Mei & Hime [28] and the same background rates scaled as described in Sec. 3.1 to represent a more realistic detector configuration at the 4850-foot level (4300 m.w.e.) of Sanford Underground Laboratory. The "Others" category includes muon capture, neutron capture on Ge and Cu, and prompt backgrounds due to cosmogenic isotopes produced *in situ*. Rates are given in ct t^{-1} y^{-1} ROI^{-1} and do not include the effects of analysis cuts.

Background	Depth	n Moderator	μ/n Veto	Total
$^*(n, n'\gamma)$	5.6	2	7.2	81
$\mathrm{Ge}(n, n)$	5.6	2	7.2	81
μ hits	5.9		10	59
Others	5.3	2	7.2	76

Table 2: Summary of the scaling factors (described in Sec. 3.1) used to derive the background rates shown in the right-hand column of Table 1. The scaling factors listed for $^*(n, n'\gamma)$ apply to all neutron inelastic scattering processes in Table 1. The factors of 7.2 reflect the combined effects of a higher veto efficiency (a factor of 1.8) and accounting for the missing EM cascades accompanying muon-induced neutrons emerging from the cavern walls in the simulations (a factor of 4).

Source	**Radioactive Isotope** [ct t^{-1} y^{-1} ROI^{-1}]			**Background** [ct t^{-1} y^{-1} ROI^{-1}]
^{enr}Ge Crystals	^{68}Ge	^{60}Co	^{232}Th / ^{238}U	<0.34
	<0.01	<0.03	<0.30	
Detector Mounts	^{208}Tl	^{214}Bi		0.06
	0.02	0.04		
Front-end Electronics	^{208}Tl	^{214}Bi		0.03
	0.01	0.02		
Cables	^{208}Tl	^{214}Bi	^{60}Co	<0.05
	0.02	0.03	<0.01	
Cryostat	^{208}Tl	^{214}Bi		0.15
	0.12	0.03		
Inner Cu Shield	^{208}Tl	^{214}Bi		0.31
	0.24	0.07		
Outer Cu Shield	^{208}Tl	^{214}Bi	^{60}Co	<0.03
	0.01	0.01	<0.01	
Pb Shield	^{208}Tl	^{214}Bi		<0.02
	<0.01	<0.01		
Other	Surface α	Rock	Other	0.11
	0.05	$\sim$ 0.05	$\sim$ 0.01	
Total Depth-independent				**$\lesssim$1.1**
Total Depth-dependent				**$\sim$0.02**
Total Background				**$\lesssim$1.1**

Table 3: Background budget for a tonne-scale detector based on simulations of a 60-kg, 57-crystal detector module in a compact shield. The depth-dependent background assumes the experiment is located at the 7400-foot level ($\sim$6600 m.w.e) of the Sanford Underground Laboratory at Homestake. The total depth-independent background rate carries an uncertainty of 30%.